



GUIDELINES FOR DESIGNING A BUSBAR WITH NOTCH FOR ALLEGRO'S CORELESS ACS37612 DIFFERENTIAL CURRENT SENSOR

By Yannick Vuillermet
Allegro MicroSystems

INTRODUCTION

The ACS37612 is a Hall-plate-based differential current sensor designed to measure current flowing in a busbar or PCB without using a ferromagnetic concentrator core. The ACS37612 is well-suited for electric vehicle applications (all-electric, hybrid, or plug-in), such as inverters, charging stations, on-board chargers, or DC links. This application note focuses on how a busbar should be designed to achieve optimum performance with this sensor.

The ACS37612 is a contactless current sensor and features differential sensing to reject common-mode stray magnetic fields. It is recommended for typical current measurement, ranging from 200 A to more than 1000 A. Due to its low-noise Hall plates, a reasonably good resolution can be achieved without the use of a ferromagnetic concentrator core. When higher accuracy is required, Allegro recommends the use of a ferromagnetic concentrator core in conjunction with A1365, A1367, or ACS70310 linear ICs.

While the ACS37612 would function using any busbar design, to achieve best performance (accuracy, high signal-to-noise ratio, high bandwidth, low sensitivity to mechanical tolerances, etc.), the busbar must include certain features. As shown in Figure 1, the ACS37612 is placed over a notch (or neckdown) in the busbar. This notch is intended to locally increase the current density and the signal measured by the IC. Note that in Figure 1, the ACS37612 is placed on top of the PCB. To reduce the distance between the Hall plates and the busbar, the ACS37612 could also be placed on the other side of the PCB. In this case, high-voltage isolation requirements should be considered.

Figure 2 illustrates how the ACS37612 senses the magnetic field induced by the current I flowing in the busbar. The ACS37612 has two Hall plates, sensitive along the Z axis and 1.87 mm away from each other. The left Hall plate measures magnetic field B_L , and the right

Hall plate measures magnetic field B_R . The output of the sensor, V_{OUT} , is proportional to the differential magnetic field, ΔB (equation 1 and equation 2). α is the ACS37612 output sensitivity to magnetic field. The relationship between the applied current and the differential field is given by the coupling factor, CF (equation 3).

$$\Delta B = B_R - B_L \quad (1)$$

$$V_{OUT} = \alpha \times \Delta B \quad (2)$$

$$\Delta B = CF \times I \quad (3)$$

Generally, a high coupling factor is preferable for good signal-to-noise ratio and high resolution. However, equation 4 indicates that coupling factor limits the maximum current range ΔI that can be measured. ΔV is the IC output range.

$$\Delta I = \Delta V / (\alpha \times CF) \quad (4)$$

Table 1 indicates all available versions of the ACS37612, including some examples of maximum currents that can be measured versus two typical system coupling factors CF. Three versions exist: 5 mV/G, 10 mV/G, and 15 mV/G. For example, the ACS37612LLUATR-010B5 version has a bipolar output, 10 mV/G sensitivity, and 5 V nominal supply. Assuming a 200 mG/A coupling factor with the busbar, the current range is ± 1000 A.

The ACS37612 is not customer programmable. Hence, once mounted in the application, it is recommended to externally rescale the output to get the desired sensitivity to current flowing in the busbar. If none of the available IC sensitivity fits the application requirements, then depending on the business case the ACS37612 can be factory-programmed to values ranging from 1 mV/G to 15 mV/G.

This application note provides guidelines on how the busbar and notch should be designed to achieve optimal performance using the ACS37612—highest signal to noise ratio and optimal use of the output range.

Note that all results in this document are derived from 3D magnetic field simulations.

Table 1

Part Number	Sensitivity α (mV/G)	Output Range ΔV (V)	Measurement Range ΔI (A)
ACS37612LLUATR-05B5	5	4.0	± 800 A with CF = 500 mG/A ± 2000 A with CF = 200 mG/A
ACS37612LLUATR-010B3	10	2.7	± 270 A with CF = 500 mG/A ± 675 A with CF = 200 mG/A
ACS37612LLUATR-010B5	10	4.0	± 400 A with CF = 500 mG/A ± 1000 A with CF = 200 mG/A
ACS37612LLUATR-015B5	15	4.0	± 267 A with CF = 500 mG/A ± 667 A with CF = 200 mG/A
ACS37612LLUATR-015U5	15	4.0	0 to 533 A with CF = 500 mG/A 0 to 1333 A with CF = 200 mG/A

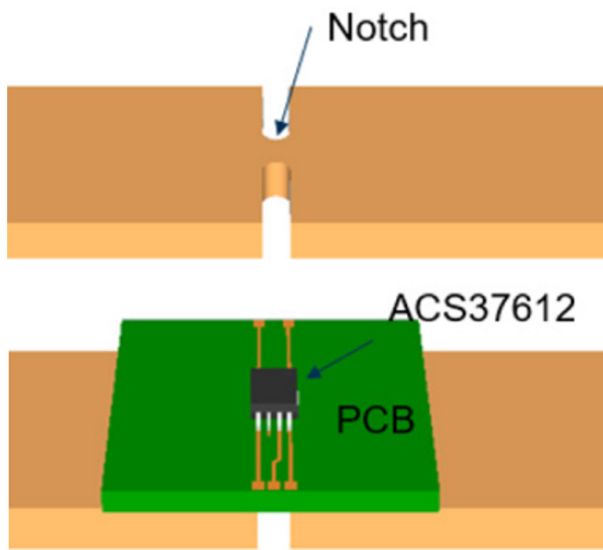


Figure 1. System overview. Top picture is busbar with rounded notch. Bottom picture shows an example of ACS37612 placement above the notch, using a PCB.

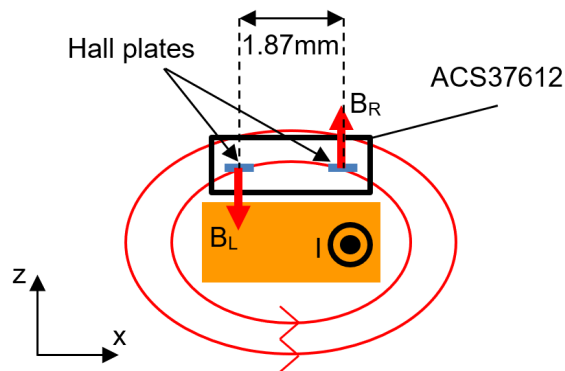


Figure 2. ACS37612 measurement principle

Thermal Considerations

This document does not focus on thermal considerations, but they must be kept in mind when designing the busbar. The thermal behavior of the complete system highly depends on the surrounding environment (heat source nearby, proximity of other materials, etc.), the cooling system (active or passive) if any, the on-time duration, and the current density flowing in the busbar.

The typical current densities used in automotive inverter applications are in the range of 10 to 30 A/mm².

The typical busbar resistance increase due to a notch is in the range of a few micro-ohms, which is small enough to not make self-heating an issue.

Busbar Design: General Information

In this section, the coupling factor and the achievable resolution will be given for various dimensions of the busbar and notch. A rounded notch is assumed in this section.

The definition of the resolution or RMS output noise δ is given in equation 5, where ϵ is the input referred noise density (2 mG_{rms}/√Hz typical for ACS37612 at room temperature), and BW is the application required bandwidth.

$$\delta = \frac{\epsilon \times \sqrt{BW \times \pi/2}}{CF} \quad (5)$$

The busbar parameters (Figure 3) are the busbar thickness T , the busbar width W , the notch width N , the notch length L and the air gap AG from the top of the busbar to the Hall plates (Figure 4). The busbar thickness T and width W are often fixed to meet the application maximum current. Therefore, the notch dimensions L and N are usually considered to adapt the coupling factor to the application specification, especially to use the full output range of the IC at maximum current.

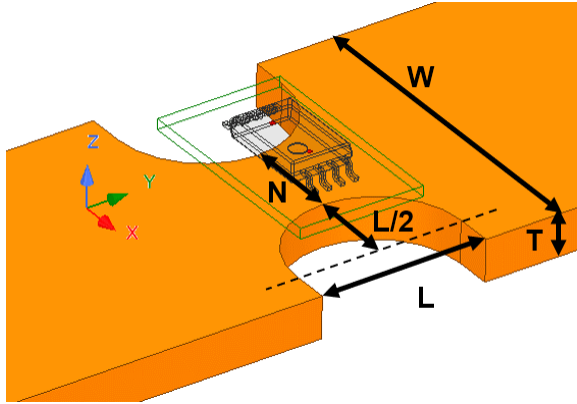


Figure 3. Busbar and notch parameters description

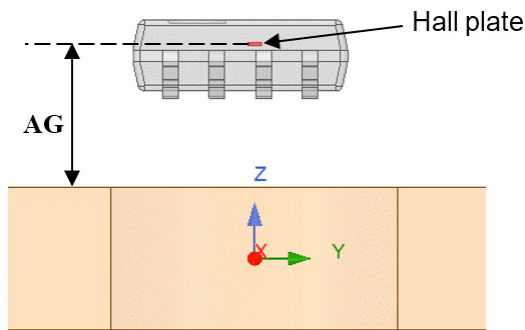


Figure 4. Air gap definition

Figure 5 shows the mapping of coupling factor versus notch length L and notch width N , with busbar thickness and width fixed to typical values ($W = 15$ mm and $T = 2$ mm). These mappings are given for three air gaps AG : 1 mm, 2 mm, and 3 mm. L appears to have low influence on coupling factor; consequently, it is recommended to keep L as small as possible to reduce notch resistivity. However, L should not be too small; otherwise, the sensitivity to IC placement could become critical. For this example, consider $L = 3$ mm as a typical value. Notch width N has a strong influence on coupling factor. And finally, coupling factor depends highly on air gap; highest coupling factors are associated with smallest air gaps.

Figure 6 shows the mapping of coupling factor versus busbar width W and notch width N , with notch length set to $L = 3$ mm and busbar thickness $T = 2$ mm. Notice that

the coupling factor does not depend much on the busbar width. Note that the white areas in the plots correspond to impossible configurations with $W < N$.

The coupling factor has much more sensitivity to busbar thickness T , as shown in Figure 7. Thinner busbars generate higher coupling factors.

Figure 8 represents the coupling factor versus air gap and versus notch width for various busbar thicknesses T , with $W = 15$ mm and $L = 3$ mm. Figure 8 is the most useful plot when designing the notch; since the coupling factor does not depend much on L and W , it allows selecting the right notch width N , from the plot corresponding to the thickness of the application busbar. Besides, the air gap (AG) is often a mechanical parameter that cannot be selected easily. The required coupling factor CF comes from equation 4 and from selected sensitivity; see SELECTING APPROPRIATE ACS37612 SENSITIVITY section.

Figure 9 shows the corresponding current resolution with 50 kHz bandwidth. This bandwidth corresponds to typical automotive inverter applications; it guarantees flat output behavior up to few kHz, corresponding to typical inverter switching frequency. The current resolution is in the range of few ampere rms. Figure 10 is similar but with 10 kHz bandwidth corresponding to typical DC applications. In this case, the resolution is 1 to 2 A_{rms} .

As a summary, when designing a busbar with a notch:

- The coupling factor has low sensitivity to notch length L and busbar width W .
- The coupling factor has high sensitivity to air gap AG , notch width N , and busbar thickness T .
- T and W are usually fixed by application requirements, especially the maximum current to be measured.
- AG is usually fixed by mechanical design and should be as low as possible.
- Short notch length L is recommended for low notch impedance.
- N is the key parameter to adapt the coupling factor to the right value.

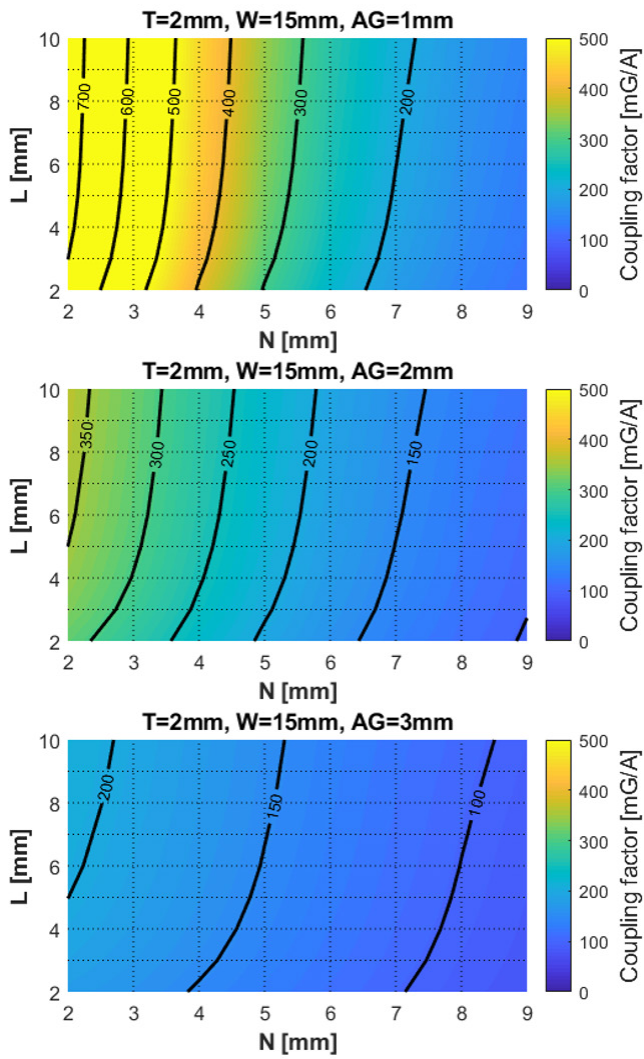


Figure 5. Coupling factor versus L and N for various air gaps
(T = 2 mm, W = 15 mm)

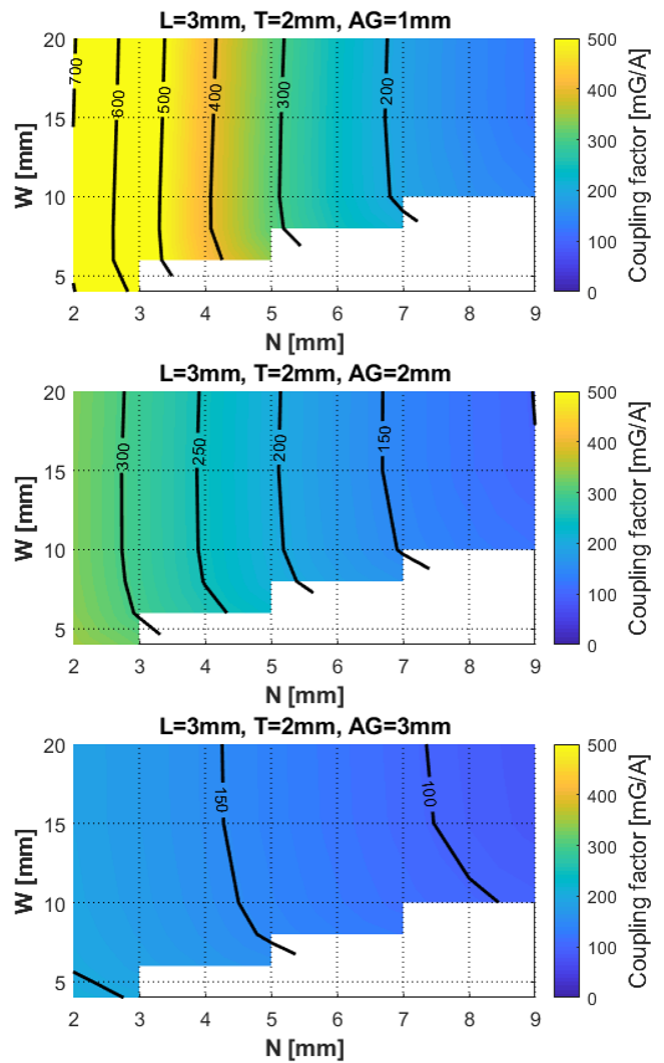


Figure 6. Coupling factor versus W and N for various air gaps
(L = 3 mm, T = 2 mm)

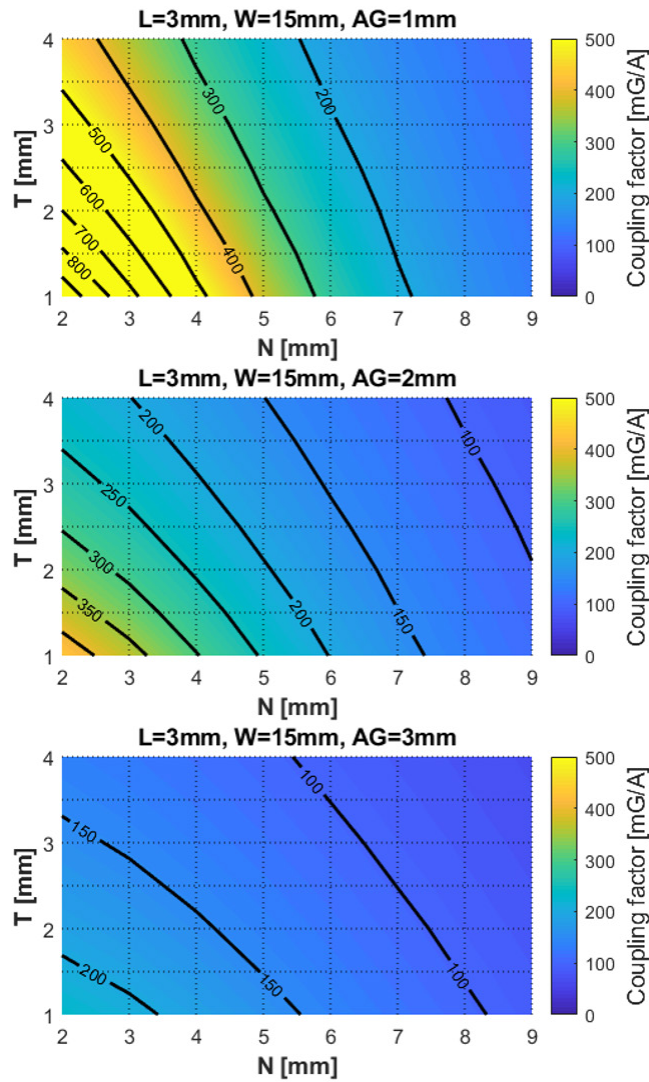


Figure 7. Coupling factor versus T and N for various air gaps (L = 3 mm, W = 15 mm)

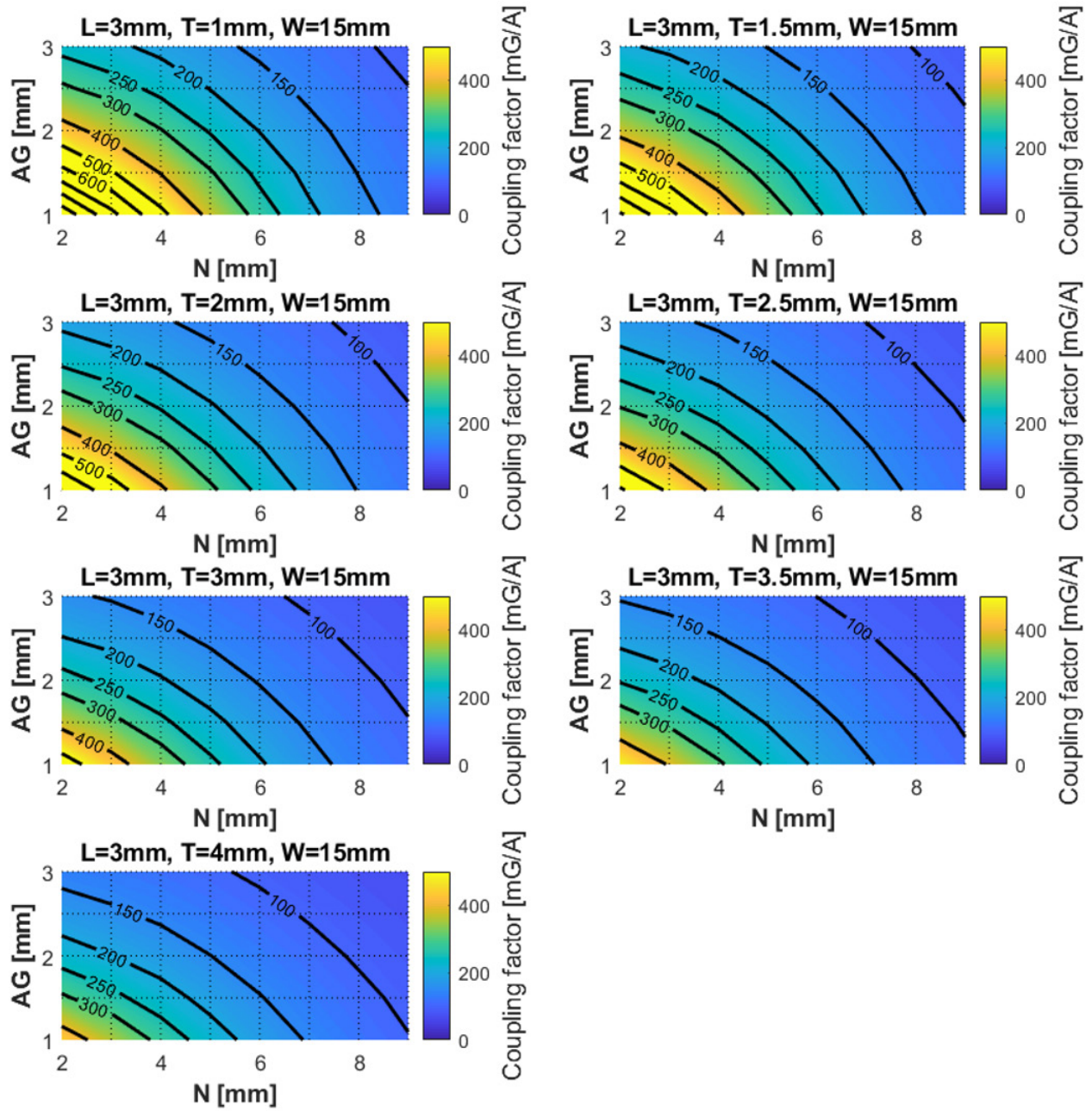


Figure 8. Coupling factor versus AG and N for various busbar thicknesses (L = 3 mm, W = 15 mm)

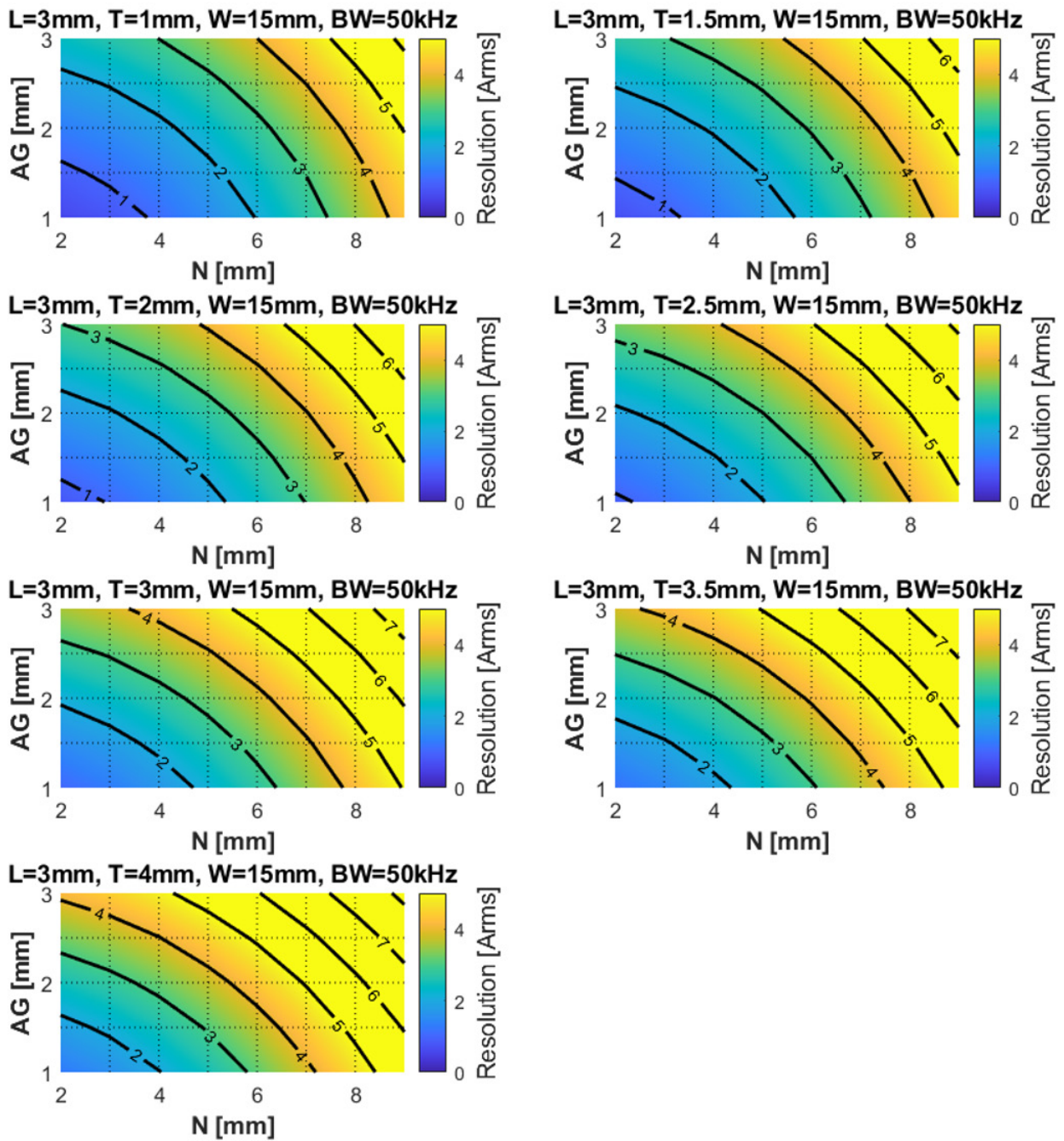


Figure 9. Resolution versus AG and N for various busbar thicknesses, at 50 kHz (L = 3 mm, W = 15 mm)

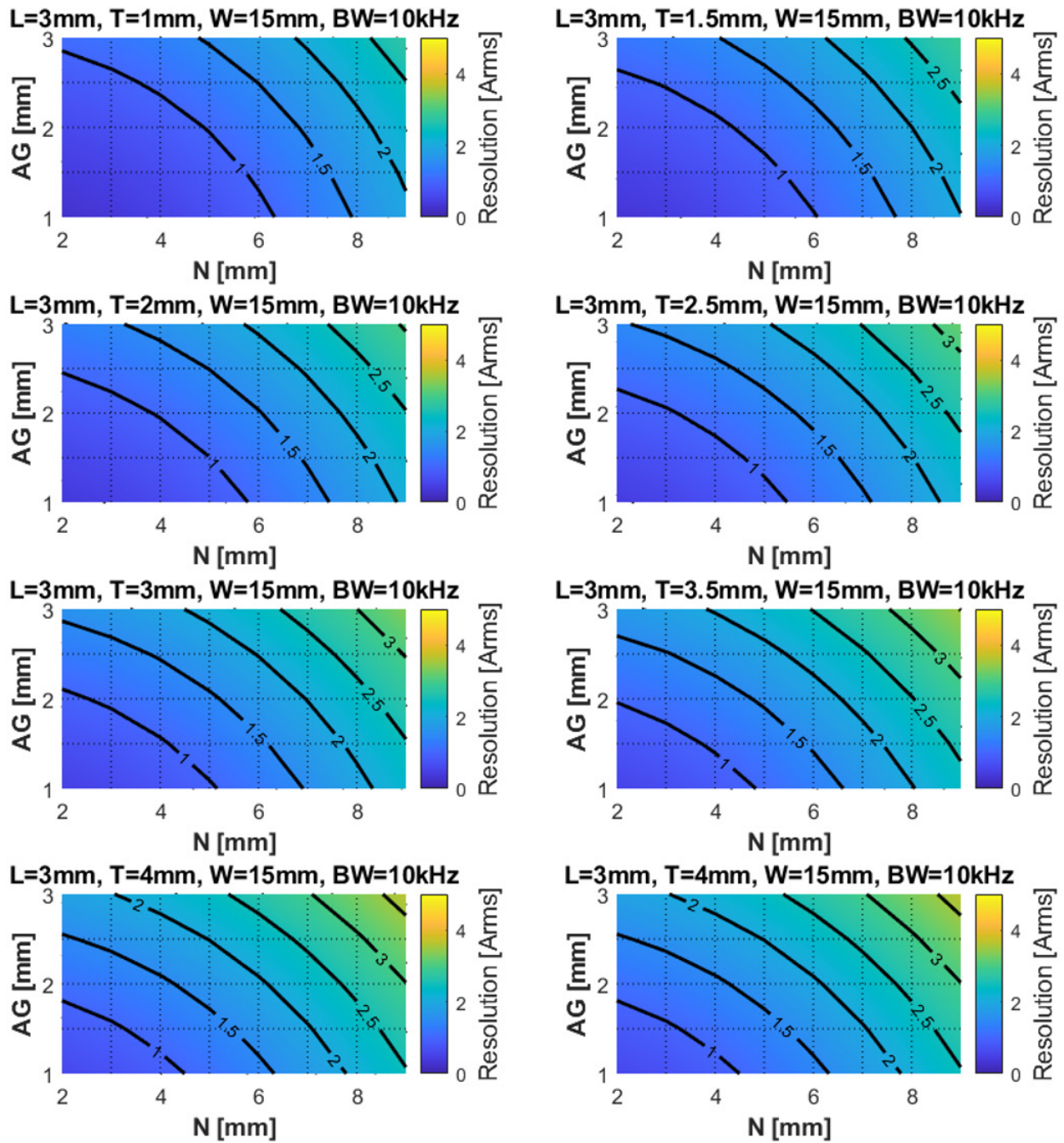


Figure 10. Resolution versus AG and N for various busbar thicknesses, at 10 kHz (L = 3 mm, W = 15 mm)

Selecting Appropriate ACS37612 Sensitivity

It is generally recommended to use the highest coupling factor and smallest sensitivity α . A high coupling factor improves the resolution (equation 5), and a small IC gain comes with better accuracy performance.

From application requirements (ΔI and ΔV) and equation 4, the procedure given in Figure 11 can be used to select the right ACS37612 sensitivity, either 5 mV/G, 10 mV/G, or 15 mV/G.

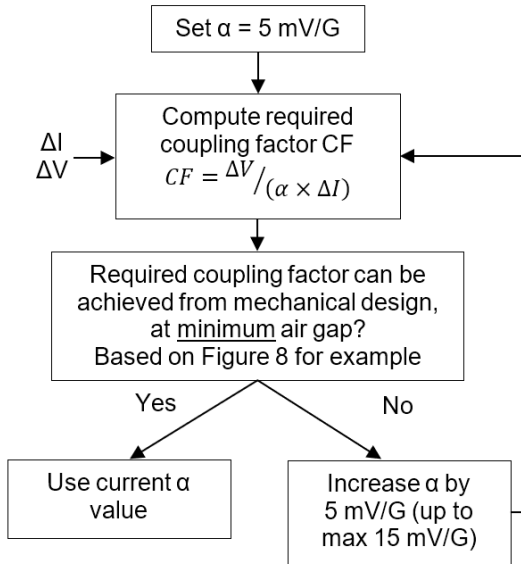


Figure 11. Procedure to select appropriate ACS37612 sensitivity

Busbar Design: An Example

For optimum busbar design, consider an application example having the following:

- Current range: ± 600 A
- Maximum current density: 20 A/mm^2
- Supply voltage: $V_{CC} = 5 \text{ V}$
- Air gap: $2.0 \text{ mm} \pm 0.5 \text{ mm}$
- Bandwidth: 50 kHz

The busbar would have $T = 2 \text{ mm}$ and $W = 15 \text{ mm}$ in order to have 20 A/mm^2 at 600 A , for example. The notch is rounded, and the length L is 3 mm . With $V_{CC} = 5 \text{ V}$, the output range is $\Delta V = 4000 \text{ mV}$. To avoid output saturation, the coupling factor should be analyzed at minimum air gap $AG = 1.5 \text{ mm}$, where the coupling factors are highest. Based on the procedure defined in Figure 11, the required coupling factor is $\sim 670 \text{ mG/A}$ (from $4000/5/1200$) with $\alpha = 5 \text{ mV/G}$. Looking at the corresponding plot in Figure 8, such a coupling factor cannot be achieved at 1.5 mm air gap. Therefore, the IC sensitivity is increased to 10 mV/G . The required coupling factor becomes $\sim 335 \text{ mV/G}$. From

Figure 8, it can be achieved with a notch width $N = 4 \text{ mm}$. Hence, 10 mV/G is the right ACS37612 sensitivity for this application. The coupling factor would go down to $\sim 200 \text{ mG/A}$ at maximum air gap $AG = 2.5 \text{ mm}$. Then, from Figure 9, the worst-case current resolution is $\sim 3 A_{\text{rms}}$ with 50 kHz bandwidth.

Sensitivity to Mechanical Tolerances

The coupling factor between the busbar and the ACS37612 is modified when the IC is not perfectly placed above the neckdown. A modification of the coupling factor directly translates into a sensitivity variation of the IC output (from equation 2 and 3).

As said before, it is recommended to rescale the output in the application once mounted in order to compensate for mounting placement error. After mounting, the coupling factor would only vary due to vibrations, thermal expansion, and/or lifetime displacement of the IC with respect to the busbar.

Left plots of Figure 12 report the coupling factor variations due to misplacement along X, Y, and Z axis, given for an $L = 3 \text{ mm}$, $T = 2 \text{ mm}$, and $W = 15 \text{ mm}$. The variations are given in percentage of the nominal placement coupling factor and for a $100 \mu\text{m}$ misplacement. For example, assuming $\pm 0.5 \text{ mm}$ placement accuracy in all three directions, the previously selected busbar ($L = 3 \text{ mm}$, $T = 2 \text{ mm}$, $W = 15 \text{ mm}$, $AG = 2 \text{ mm}$, and $N = 4 \text{ mm}$) would see coupling factor variations of -2.5% ($\approx -0.5 \times 5$) along X, $+1.5\%$ ($\approx -0.3 \times 5$) along Y, and -22.5% ($\approx -4.5 \times 5$) along Z.

The misplacement along Z, i.e. air gap, appears to be the most critical tolerance, especially with thin width (small N). The air gap variations must be well-controlled in the application with respect to vibrations, thermal expansion, and lifetime displacement to use the ACS37612 in an optimal manner.

From a general point of view, the sensitivity tolerance to misplacements is smaller with larger neckdown.

Right plots of Figure 12 report the coupling factor variations due to an IC tilt around X, Y, and Z axis, given for an $L = 3 \text{ mm}$, $T = 2 \text{ mm}$, and $W = 15 \text{ mm}$. The variations are given in percentage of the nominal coupling factor and for a 1° tilt. These plots demonstrate that the coupling factor is sensitive to IC tilts but does not depend much on air gap and notch width. The most critical tilt is around y axis.

For example, assuming $\pm 3^\circ$ tilt in all three directions, the notch from the example design would see coupling factor variations of -0.3% ($\approx -0.1 \times 3$) around X, -0.9% ($\approx -0.3 \times 3$) around Y, and -0.3% ($\approx -0.1 \times 3$) around Z.

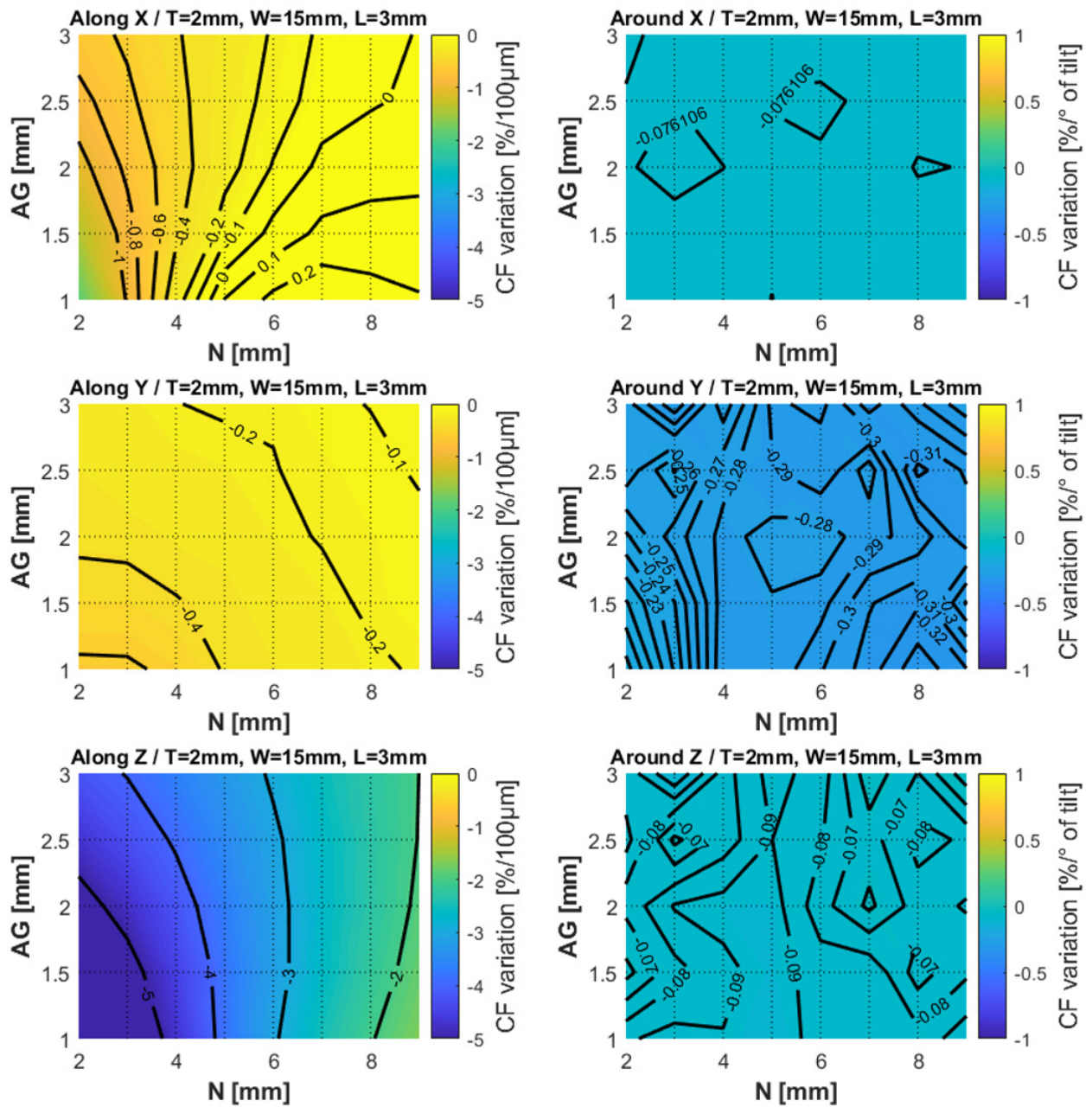


Figure 12. Coupling factor variations due to displacement along x, y, and z axis and rotation around x, y, and z (L = 3 mm, T = 2 mm, and W = 15 mm)

Behavior Over Frequency

All results discussed so far have assumed a continuous DC current flowing in the conductor. When an AC current is driven in the busbar, eddy currents are generated in this busbar. They tend to modify the current distribution inside the conductor; from a uniform density at low frequency, the density becomes higher near the surface of the conductor at high frequency (Figure 13).

These variations of the current density modify the magnetic field distribution around the notch. Therefore, the differential magnetic field measured by the ACS37612 in AC is altered compared to the magnetic field measured with a DC current. It implies a variation of the coupling factor (Figure 14) and a phase delay (Figure 15) in the measurements. For example, at 2 mm air gap, the coupling factor loss in the previously design notch ($N = 4$ mm) would be around -1% at 1 kHz and -20% at 10 kHz. Meanwhile, the magnetic signal lags the current by -3° elec at 1 kHz and -13° elec at 10 kHz.

The coupling factor variations due to AC current are small over air gap but large versus notch width N and current frequency. From a design point of view, it is recommended to use the smallest notch as possible to reduce eddy current effect. Indeed, with a smaller notch, there is less room for the eddy current to significantly modify a uniform current density. Despite not being reported here, the same

applies to the thickness of the busbar—a thinner busbar is less sensitive to eddy current effects. One may want to reduce the busbar thickness, T , and increase busbar width, W , when high frequency currents (or fast transients) are to be measured.

It should be noted that most of the time, the bandwidth of the current measurement is not limited by the ACS37612 bandwidth (150 kHz) but instead by the eddy current in the busbar.

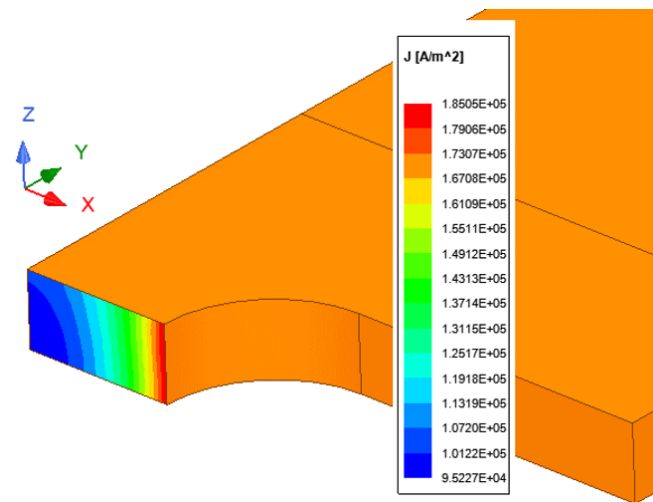


Figure 13. Current density inside the notch at 2 kHz ($L = 3$ mm, $N = 4$ mm, $T = 2$ mm, $W = 15$ mm). Only a portion (one quarter) of the busbar is shown due to symmetries.

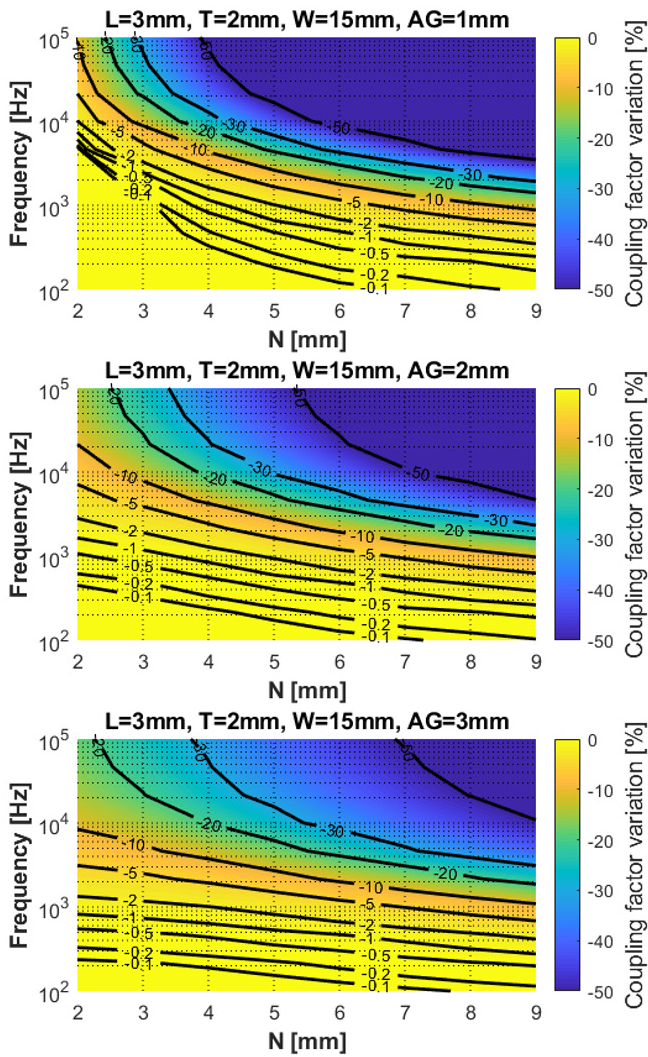


Figure 14. Coupling factor variation over frequency, due to eddy current in the busbar ($L = 3\text{ mm}$, $T = 2\text{ mm}$, $W = 15\text{ mm}$)

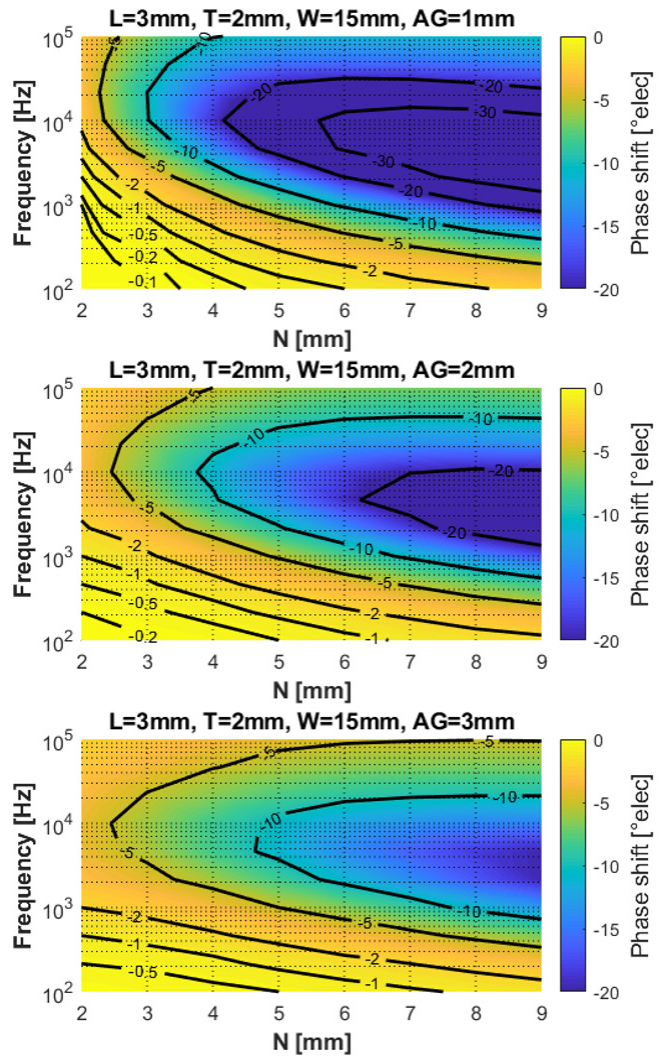


Figure 15. Phase delay over frequency, due to eddy current in the busbar ($L = 3\text{ mm}$, $T = 2\text{ mm}$, $W = 15\text{ mm}$)

Influence of Notch Shape

In this section, the coupling factors of a rounded notch and a straight notch (Figure 16) are compared (Figure 17). The differences are very small between these two shapes—the straight notch has slightly more coupling factor for a given configuration. Consequently, choosing between a rounded or a straight busbar should be a mechanical decision more than an electromagnetic decision.

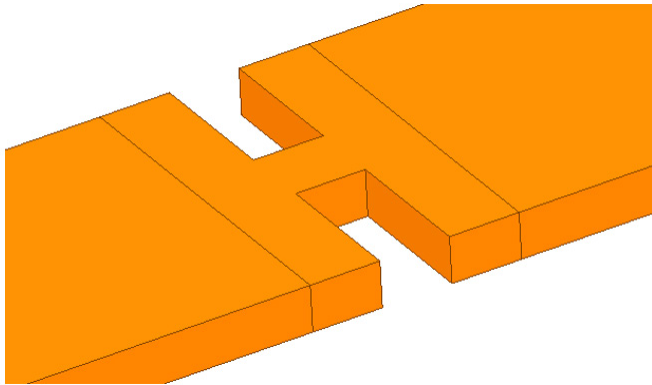


Figure 16. Straight notch view

Conclusions

This application note offers guidelines for achieving optimum busbar and notch designs using the Allegro ACS37612 coreless current sensor. When well-designed, current ranges from two hundred amperes to more than one thousand amperes can be measured with a reasonably good resolution of a few ampere with a typical 50 kHz bandwidth.

The key parameters for the notch design are:

- Air gap: Set to minimum to guarantee good current resolution. In addition, ACS37612 intrinsic principle makes it sensitive to air gap tolerances; it is recommended to use this IC in an environment where air gap is well-controlled during operation (vibration, thermal expansion, aging).
- Notch width: Use to adjust the coupling factor in order to use the full output range of ACS37612. Notch width selection also results from a compromise between signal level, thermal effect, and bandwidth.

Contact an Allegro representative for any further questions or support.

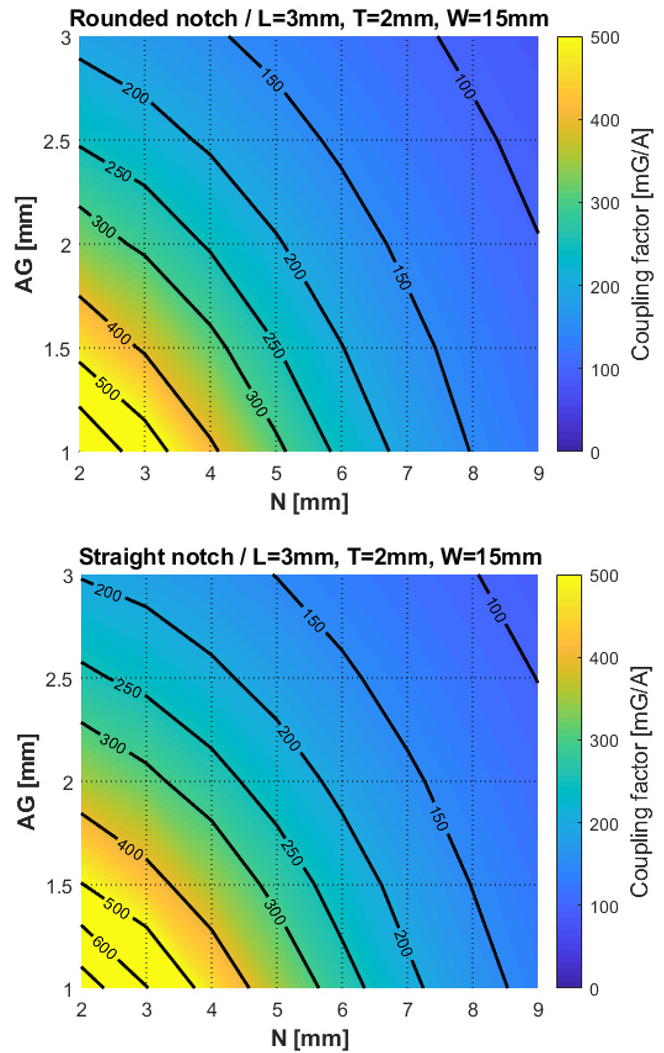


Figure 17. Coupling factor with rounded and straight notch
($L = 3 \text{ mm}$, $T = 2 \text{ mm}$, $W = 15 \text{ mm}$)

Revision History

Number	Date	Description	Responsibility
-	February 21, 2020	Initial release	Y. Vuillermet
1	October 26, 2021	Updated figure 2	Y. Vuillermet

Copyright 2021, Allegro MicroSystems.

The information contained in this document does not constitute any representation, warranty, assurance, guaranty, or inducement by Allegro to the customer with respect to the subject matter of this document. The information being provided does not guarantee that a process based on this information will be reliable, or that Allegro has explored all of the possible failure modes. It is the customer's responsibility to do sufficient qualification testing of the final product to ensure that it is reliable and meets all design requirements.

Copies of this document are considered uncontrolled documents.